Analysis of the inverse problem for determining nematic liquid crystal director profiles from optical measurements using singular value decomposition.

Lionheart, WRB and Newton, CJP

2006

MIMS EPrint: **2006.420**

Manchester Institute for Mathematical Sciences
School of Mathematics

The University of Manchester

Reports available from: http://eprints.maths.manchester.ac.uk/
And by contacting: The MIMS Secretary
School of Mathematics
The University of Manchester
Manchester, M13 9PL, UK

ISSN 1749-9097

Analysis of the inverse problem for determining nematic liquid crystal director profiles from optical measurements using singular value decomposition.

W. R. B. Lionheart[1] **and C. J. P. Newton**[2]

[1] School of Mathematics, University of Manchester, P.O. Box 88, Manchester M60 1QD, United Kingdom

[2]Hewlett-Packard Laboratories, Filton Road, Stoke Gifford, Bristol BS34 8QZ, United Kingdom

E-mail: `Bill.Lionheart@manchester.ac.uk, chris.newton@hp.com`

Abstract. We use the problem of determining nematic liquid crystal director profiles from optical measurements as an example to illustrate that what is often treated purely as a data fitting problem is really an inverse problem and that useful insights can be obtained by treating it in this way. Specifically we illustrate the analysis of the sufficiency of data and the sensitivity of a solution to measurement errors. We assume a stratified medium where the Berreman method can be used for the optical forward problem and we consider the inverse problem to be the determination of an anisotropic dielectric permittivity tensor from optical data. A numerical Singular Value Decomposition (SVD) analysis reveals that although this inverse problem is severely ill-conditioned it is possible to determine depth-dependent information provided the medium is sufficiently birefringent and that, as one might expect, a larger range of incident angles gives greater information. Analytical solutions of the Berreman equations for general perturbations of an orthorhombic crystal confirm uniqueness of solution for the linearized problem and give further insights into the severely ill-posed nature of the inverse problem.

PACS numbers: 02.30.Zz, 42.70.Df

1. Introduction

Many inverse problems occur in experimental physics, although these are often just treated as data fitting problems, where the parameters in a forward model are varied until a good fit to the experimental data is obtained. Examples include optically probing nematic liquid crystal cells to obtain information about the director profile through the cell (the example used here to illustrate the approach being presented) and determining material structure using X-rays, or neutron scattering. In these problems some initial questions that arise are:

(i) Can the required parameters be deduced from the data?

(ii) How is the solution affected by the amount and type of data collected?

(iii) How can a solution be efficiently obtained?

(iv) How does experimental noise in the data limit the information that we can reliably deduce from it?

These questions are typical of many such inverse problems that occur in experimental physics and where a similar analysis to that given here may also be appropriate.

Nematic liquid crystals are generally made up of rod-like molecules which show a nematic phase, i.e. a phase where the centres of mass of the molecules have no positional order, but where there is local orientational order. At any point, $\mathbf{r}$, in the material we can define an average direction, which we represent by a unit vector, $\mathbf{n}(\mathbf{r})$ and which we call the director. We make no distinction between $\mathbf{n}(\mathbf{r})$ and $-\mathbf{n}(\mathbf{r})$. In the absence of external influences the liquid crystal (LC) director is the same everywhere, there is no distortion. In an LC cell the cell walls are treated to provide boundary conditions that the director must satisfy. The LC takes up a configuration which minimizes the free energy, which in its simplest form (with rigid anchoring at the boundaries and no applied fields) is given in 1. The three terms in the integral represent the allowable distortions for a nematic LC: splay, twist and bend.

$$F = \int_V \left[\frac{1}{2} K_{11} \left(\nabla \cdot \mathbf{n} \right)^2 + \frac{1}{2} K_{22} \left(\mathbf{n} \cdot \left(\nabla \wedge \mathbf{n} \right) \right)^2 + \frac{1}{2} K_{33} \left| \mathbf{n} \wedge \left(\nabla \wedge \mathbf{n} \right) \right|^2 \right] dv \qquad (1)$$

These are given the elastic constants K_{11}, K_{22} and K_{33}. These can be measured experimentally and are typically of the order of $10^{-11} Nm^{-2}$.

Optically probing nematic liquid crystal cells, although experimentally straightforward, relies on difficult data fitting to give the director profile [1, 2, 3, 4]. Work at Hewlett Packard Laboratories, Bristol (HPLB) is focused on developing a technique that can efficiently obtain director profiles for such cells to allow different surface treatments and LC materials to be evaluated.

The experimental set-up uses a polarimeter to measure the normalized Stokes parameters [5] of monochromatic light transmitted by a test cell as a function of the incident angle and polarization state of the input beam. The data is then compared to results obtained from an optical model of the system and the model parameters adjusted to give a good fit to the data.

In this paper results are presented in terms of the fundamental model parameters, the elements of the dielectric tensor.

2. Experimental method

Figure 1 shows the experimental setup used at HPLB. A cylindrical mount enables data to be collected over a wide range of incident angles. For each incident angle normalized Stokes parameters are measured for a number of input polarisations‡. For the Stokes parameter measurement the z-axis is taken to be in the direction of the beam and the alignment of the polarimeter defines the x and y-axes. In the experimental setup used at HPLB the x-axis is horizontal and the y-axis vertical and into the optical bench. Similar experiments are carried out in the Department of Physics at the University of

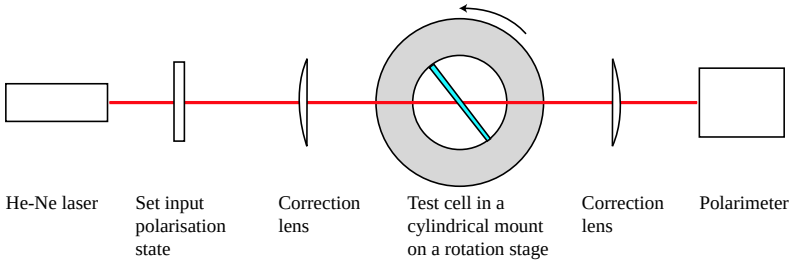

Figure 1. The experimental setup used at HPLB. The correction lenses ensure that the beam is collimated on the cell. The polarimeter used gives normalized Stokes parameters.

Exeter. Later in this paper we will apply the same techniques to their experimental setup.

3. The forward problem

The forward problem is the calculation of the Stokes parameters for a given incident angle and input polarization.

Taking the z-axis in the direction of the beam and defining the x and y-axes relative to the laboratory system the electric field vector, $\mathcal{E}$, can be written $\mathcal{E} = (\mathcal{E}_{\mathbf{x}}, \mathcal{E}_{\mathbf{y}})^{\mathbf{T}}$ (where T denotes the transpose) with $\mathcal{E}_x = a\cos(\omega t - kz)$ and $\mathcal{E}_y = b\cos(\omega t - kz + \delta)$. The Stokes parameters [5] are defined as

$$S_0 = a^2 + b^2,\ S_1 = a^2 - b^2,\ S_2 = 2ab\cos\delta \ \text{ and}$$
$$S_3 = 2ab\sin\delta \tag{2}$$

To calculate the $\mathcal{E}$-vector we use the Berreman 4×4 matrix method [6]. This method supersedes the simpler 2×2 Extended Jones method [7] used elsewhere in that reflected waves are also correctly included.

‡ Typically four input polarizations are used: linear polarization at 22.5^o, 67.5^o and 112.5^o to the horizontal (the x-axis) and left handed circular polarization.

Maxwell's equations (in SI units) for a dielectric are[8]

$$\nabla \cdot \mathbf{D} = 0 \tag{3}$$
$$\nabla \cdot \mathbf{B} = 0 \tag{4}$$
$$\nabla \wedge \mathbf{E} = -\frac{\partial \mathbf{B}}{\partial t} \tag{5}$$
$$\nabla \wedge \mathbf{H} = \frac{\partial \mathbf{D}}{\partial t} \tag{6}$$

Putting $(x, y, z) = (x_1, x_2, x_3)$ we write each of the terms in the solution as

$$\mathbf{U} = \mathcal{U}(z) exp(\mathrm{i}(\omega t - k_1 x_1 - k_2 x_2)) \tag{7}$$

giving

$$\begin{aligned}
\mathrm{i}\omega\mathcal{D}_1 &= -\mathrm{i}k_2\mathcal{H}_3 - \frac{\partial \mathcal{H}_2}{\partial x_3} \\
\mathrm{i}\omega\mathcal{D}_2 &= \mathrm{i}k_1\mathcal{H}_3 + \frac{\partial \mathcal{H}_1}{\partial x_3} \\
\mathrm{i}\omega\mathcal{D}_3 &= -\mathrm{i}k_1\mathcal{H}_2 + ik_2\mathcal{H}_1 \\
\mathrm{i}\omega\mathcal{B}_1 &= \mathrm{i}k_2\mathcal{E}_3 + \frac{\partial \mathcal{E}_2}{\partial x_3} \\
\mathrm{i}\omega\mathcal{B}_2 &= -\mathrm{i}k_1\mathcal{E}_3 - \frac{\partial \mathcal{E}_1}{\partial x_3} \\
\mathrm{i}\omega\mathcal{B}_3 &= \mathrm{i}k_1\mathcal{E}_2 - ik_2\mathcal{E}_1
\end{aligned} \tag{8}$$

We assume that $\mathcal{D}$ is linearly related to $\mathcal{E}$ and that $\mathcal{B}$ is linearly related to $\mathcal{H}$ with relative permeability $\mu = 1$ and write§

$$\mathcal{D} = \epsilon_0 \epsilon \mathcal{E} \tag{9}$$
$$\mathcal{B} = \mu_0 \mathcal{H} \tag{10}$$

Choosing our co-ordinate system so that the xz-plane is the incident plane ($k_2 = 0$) and substituting for $\mathcal{D}$ and $\mathcal{B}$ gives‖

$$\begin{aligned}
\mathrm{i}\omega\epsilon_0\epsilon_{1k}\mathcal{E}_k &= -\frac{\partial \mathcal{H}_2}{\partial x_3} \\
\mathrm{i}\omega\epsilon_0\epsilon_{2k}\mathcal{E}_k &= \mathrm{i}k_1\mathcal{H}_3 + \frac{\partial \mathcal{H}_1}{\partial x_3} \\
\mathrm{i}\omega\epsilon_0\epsilon_{3k}\mathcal{E}_k &= -\mathrm{i}k_1\mathcal{H}_2 \\
\mathrm{i}\omega\mu_0\mathcal{H}_1 &= \frac{\partial \mathcal{E}_2}{\partial x_3} \\
\mathrm{i}\omega\mu_0\mathcal{H}_2 &= -\mathrm{i}k_1\mathcal{E}_3 - \frac{\partial \mathcal{E}_1}{\partial x_3} \\
\mathrm{i}\omega\mu_0\mathcal{H}_3 &= \mathrm{i}k_1\mathcal{E}_2
\end{aligned} \tag{11}$$

§ In SI units $\epsilon_0 c^2 = 10^7/4\pi$ (by definition) and $\mu_0\epsilon_0 c^2 = 1$. ϵ is the dielectric tensor.
‖ We use the normal summation convention, i.e. we sum over repeated indices. So, for example, $\epsilon_{1k}\mathcal{E}_k = \epsilon_{11}\mathcal{E}_1 + \epsilon_{12}\mathcal{E}_2 + \epsilon_{13}\mathcal{E}_3$.

$k_1 = (\omega/c)\xi$, were ξ depends on the incident angle and the refractive index of the input medium (usually air). Eliminating $\mathcal{E}_3$ and $\mathcal{H}_3$ gives an ordinary differential equation for the Berreman field vector $X = (\mathcal{E}_1, \mathcal{H}_2, \mathcal{E}_2, -\mathcal{H}_1)^T$

$$\frac{\partial}{\partial x_3} X = -\frac{\mathrm{i}\omega}{c} M X \tag{12}$$

where the matrix M is

$$M = \begin{pmatrix} -\frac{\epsilon_{13}}{\epsilon_{33}}\xi & \mu_0 c \frac{\epsilon_{33}-\xi^2}{\epsilon_{33}} & -\frac{\epsilon_{23}}{\epsilon_{33}}\xi & 0 \\ \epsilon_o c\left(\epsilon_{11} - \frac{{\epsilon_{13}}^2}{\epsilon_{33}}\right) & -\frac{\epsilon_{13}}{\epsilon_{33}}\xi & \epsilon_0 c\left(\epsilon_{12} - \frac{\epsilon_{13}\epsilon_{23}}{\epsilon_{33}}\right) & 0 \\ 0 & 0 & 0 & \mu_0 c \\ \epsilon_0 c\left(\epsilon_{12} - \frac{\epsilon_{13}\epsilon_{23}}{\epsilon_{33}}\right) & -\frac{\epsilon_{23}}{\epsilon_{33}}\xi & \epsilon_0 c\left(\epsilon_{22} - \frac{\epsilon_{23}^2}{\epsilon_{33}} - \xi^2\right) & 0 \end{pmatrix} \tag{13}$$

The final value problem for this linear ODE can be solved to give the linear relationship between 'initial data' $X(0)$ and $X(z) = P(z)X(0)$, where $P(z)$ is a propagation matrix. Given the field vector in the input plane we can calculate the field vector at the output ($z = d$). We will write $P(d)$ as simply P. We now assume that we have an input wave, X_i, a reflected wave, X_r and a transmitted wave, X_t. We then have

$$X_t = P(X_i + X_r) \tag{14}$$

This equation can be re-arranged (see Appendix 9) to give X_r and X_t as functions of the input field vector, X_i.

For a region where M is independent of z we write each of the terms in the solution as

$$\mathcal{U}(z) = \mathcal{U} exp(-\mathrm{i}(\omega/c)\eta z) \tag{15}$$

and Berreman's equation (12) then reduces to an eigenvalue equation

$$MX = \eta X \tag{16}$$

The eigen-solutions of this equation give the modes that propagate in that region.

4. Linearization and the SVD

In this case the specific questions that we would like to answer are:

(i) Can the dielectric tensor through the cell be deduced from the data?

(ii) How is the solution affected by the range of incident angles and input polarizations used?

(iii) Given the limited accuracy of the polarimeter how much information can be deduced from the data?

As a first step to answering these questions we have carried out an analysis of the inverse problem by linearization and using singular value decomposition (SVD). The SVD is a widely used tool in inverse problems as it can be used to study the number of unknown parameters one can expect to reliably recover from a given system of measurements of a specified precision. The Truncated SVD (TSVD) gives an explicit inversion of a

linearized problem ignoring components in the solution that are not justified by the precision of the data.

The forward problem can be written as

$$S = F(p) \tag{17}$$

with S the vector of measured Stokes parameters, and F the corresponding calculated values for the vector of model parameters p. We wish to solve the inverse problem i.e. given a set of measured Stokes parameters find the model parameters consistent with this data. This inverse problem is *ill-posed* in the sense that without including additional a priori information widely varying parameter values will fit the data to a given precision. To understand this difficulty we first linearize the problem about some initial guess for the parameters p_0

$$S = F(p_0) + J\delta p \tag{18}$$

giving

$$J\delta p = S - F(p_0) = \delta S \tag{19}$$

where J is the Jacobian matrix, $J_{ij} = \partial S_i/\partial p_j$.

A solution to the (non-linear) inverse problem is obtained by iteratively solving the linearized problem and updating the model parameters. Given an initial set of parameters, p_0 we obtain the next estimate by solving the equation

$$J\delta p = \delta S \tag{20}$$

for δp. Solution of this equation is ill-conditioned and the results strongly affected by any noise in the data. To investigate this we look at the SVD of the Jacobian, J.

Any $m \times n (m \geq n)$ real matrix J can be written [9] as

$$J = U\Sigma V^T \tag{21}$$

where

U is an $m \times m$ orthogonal matrix (its column vectors, u_i, are orthonormal).

V is an $n \times n$ orthogonal matrix (with column vectors, v_i. V^T is the transpose of V).

Σ is an $m \times n$ matrix, arranged so that the upper $n \times n$ block is diagonal with these diagonal elements in descending order, and zeros elsewhere. The $m - n$ rows below are all zeros. We will also write this as $\Sigma = \mathrm{diag}(\sigma_1, \ldots, \sigma_n)$. The σ_i are called singular values. If $\mathrm{rank}(J) = r$ then the last $(n - r)$ singular values will be zero and we will write $\Sigma = \mathrm{diag}(\sigma_1, \ldots, \sigma_r, 0, \ldots, 0)$

This is the SVD of the matrix. Given this decomposition we can write the least-squares solution of (20) as

$$\delta p = \sum_{i=1}^{r} \frac{u_i^T \delta S}{\sigma_i} v_i \tag{22}$$

Small singular values give large contributions to the solution vector and this is where the ill-conditioning arises. A measure of this ill-conditioning is the ratio of the largest to the

smallest singular value, the condition number of the matrix [10]. Any noise on the data carries across to δS and is then amplified by the smaller singular values. Put another way, if we only know the data δS to some limited relative precision ε, we are not justified in recovering components of the parameter vector $u_i^T \delta p$ for $\sigma_i/\sigma_1 < \varepsilon$. The graph of the decay of the singular values can therefore be used to indicate how many independent components of δp we can expect to recover for a given measurement precision. We can see how this varies for different data sets and choices of parametrization. The TSVD is an approximate least squares solution where the sum in (22) is taken only as far as some $k < \min(m, n)$ determined by the accuracy of the data.

5. Numerical results

Because the dielectric tensor is symmetric we need 6 parameters to specify it completely. For N layers we have $6N$ parameters in all. For the results given below the Jacobian is

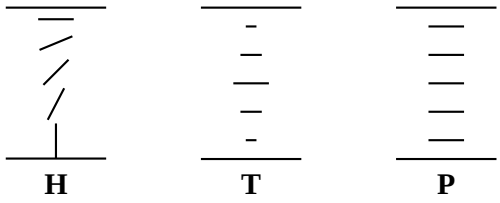

Figure 2. The director profiles used in the numerical tests (projected onto the xz plane).

calculated for sets of initial parameters (p_0) calculated by assuming that the dielectric tensor is derived from an LC layer and that the LC director in this layer is aligned in the following ways (see figure 2):

H The director is parallel to the incident (xz) plane. It is parallel to the z-axis at $z = 0$, and is parallel to the x-axis at $z = d$ (d is the thickness of the cell). The tilt of the director varies linearly across the cell. A hybrid aligned nematic (HAN) cell. This configuration closely models the experimental set-up at HPLB¶.

T The director is parallel to the xy-plane and is aligned at $-\pi/4$ to the x-axis at $z = 0$ and twists linearly through the cell so that it is aligned at $\pi/4$ to the the x-axis at $z = d$. A twist cell with no pre-tilt.

P The director is parallel to the x-axis throughout the cell. A planar cell with no pre-tilt.

In order to focus on the LC layer of the cell we choose the ordinary and extraordinary refractive indices (n_o and n_e) so that their average is equal to the refractive index of the surrounding medium (glass)$^+$. The LC is further assumed to be lossless so

¶ For a real material the director does not vary linearly, the amount of this non-linearity is small and depends on the ratio of the bend and splay elastic constants.

$^+$ This is probably a worst case situation as it minimizes any reflections and the resulting fringes in the data. The fringes in the data provide strong features which aid the fitting process.

its refractive index is real. Given the refractive indices and the azimuthal (ϕ) and tilt (θ) angles of the director the elements of the dielectric tensor are given by

$$\begin{aligned}
\epsilon_{11} &= n_o^2 + (n_e^2 - n_o^2)\cos^2\theta\cos^2\phi \\
\epsilon_{12} = \epsilon_{21} &= (n_e^2 - n_o^2)\cos^2\theta\sin\phi\cos\phi \\
\epsilon_{13} = \epsilon_{31} &= (n_e^2 - n_o^2)\cos\theta\sin\theta\cos\phi \\
\epsilon_{22} &= n_o^2 + (n_e^2 - n_o^2)\cos^2\theta\sin^2\phi \\
\epsilon_{23} = \epsilon_{32} &= (n_e^2 - n_o^2)\cos\theta\sin\theta\sin\phi \\
\epsilon_{33} &= n_o^2 + (n_e^2 - n_o^2)\sin^2\theta
\end{aligned} \tag{23}$$

The LC layer is modelled as an infinite plane in (x, y) divided into N uniform anisotropic layers normal to the z-axis and of equal thickness (N is typically 50). For each test director profile (H, T or P) we calculate the azimuthal (ϕ) and tilt (θ) angles of the director in the centre of the layer and use these to calculate the dielectric tensor for this layer.

Unless otherwise stated, for the numerical results presented here: the birefringence, $\Delta n = n_e - n_o$, was fixed at 0.15 (a typical value for liquid crystals); the incident angles were in the range -70 to $+70$ degrees and the number of Stokes vectors was kept constant (there were 200 incident angles and four different input polarizations - linear polarization at 22.5, 67.5 and 112.5 degrees to the x-axis, and left circular polarization).

Figure 3 shows how the normalized singular values, σ_i/σ_1, vary with N, the number

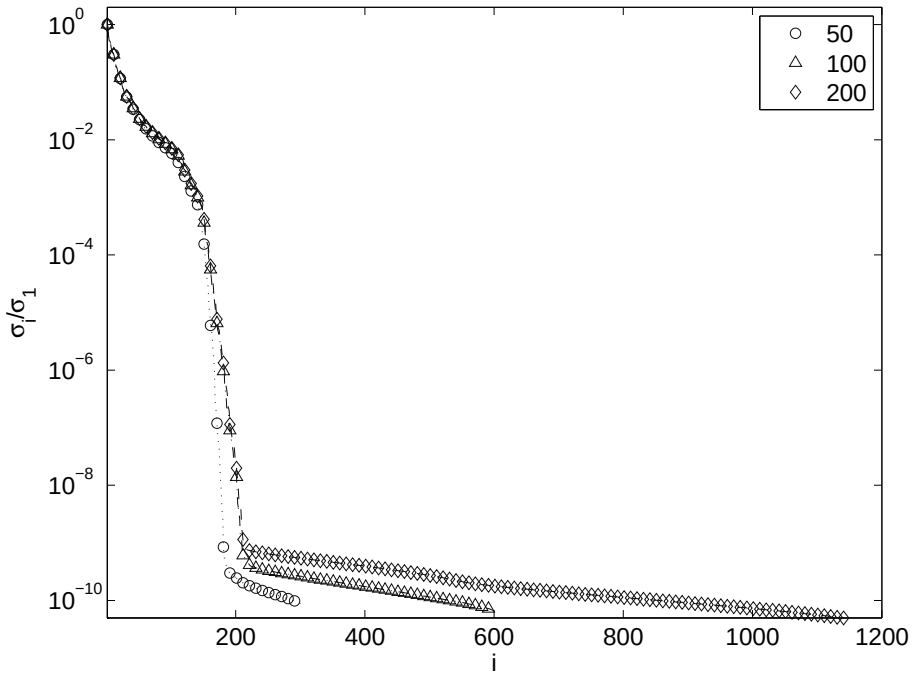

Figure 3. The normalised singular values, σ_i/σ_1, for three different numbers of layers, $N = 50, 100$ and 200.

of layers in the system*. As the number of layers increases so does the number of parameters. However there is no significant change in the number of singular vectors that can usefully be used to construct a solution (those for which $\sigma_i/\sigma_1 < \varepsilon$). For the other results presented here we will therefore use $N = 50$.

Figure 4 shows how the normalized singular values depend on the initial parameters,

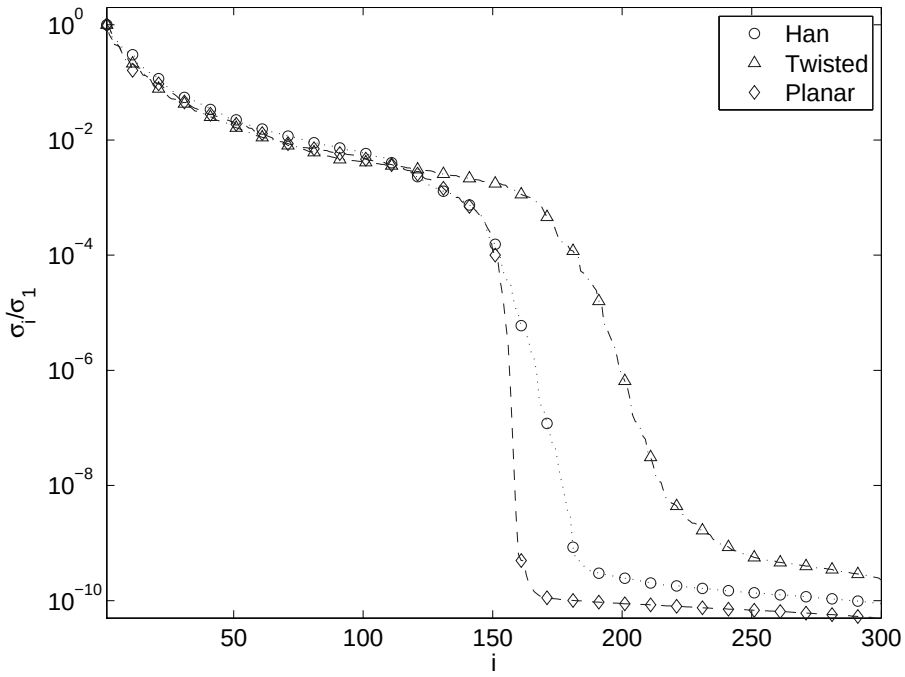

Figure 4. The normalised singular values, σ_i/σ_1, for different initial parameter configurations, p_0.

p_0. For $\sigma_i/\sigma_1 > 0.01$ we see that the normalized singular values show little dependence on the initial parameter set, although, of course, the corresponding singular vectors may be quite different. For the other results presented below we just use the HAN-like profile.

In the photoelastic tomography of a stratified medium when measuring only rays passing through all layers, extra input rays in the same incident plane give no further information (although they may increase the signal to noise ratio). It might be imagined that the same thing applies in this case. Figure 5 shows how the normalized singular values vary with different incident angle ranges. As the angle range increases we do see a marked increase in the number of singular vectors that we can use to construct a solution. Why this difference? In photoelastic tomography [16] the birefringence is weak and the ray approximation can be used to reduce the forward problem to a Radon transform along rays of the component of the permittivity tensor perpendicular to the rays. This shows why extra rays passing through all layers (as they must in this case) give no extra

* For clarity, unless otherwise stated, markers are only plotted every 10 points.

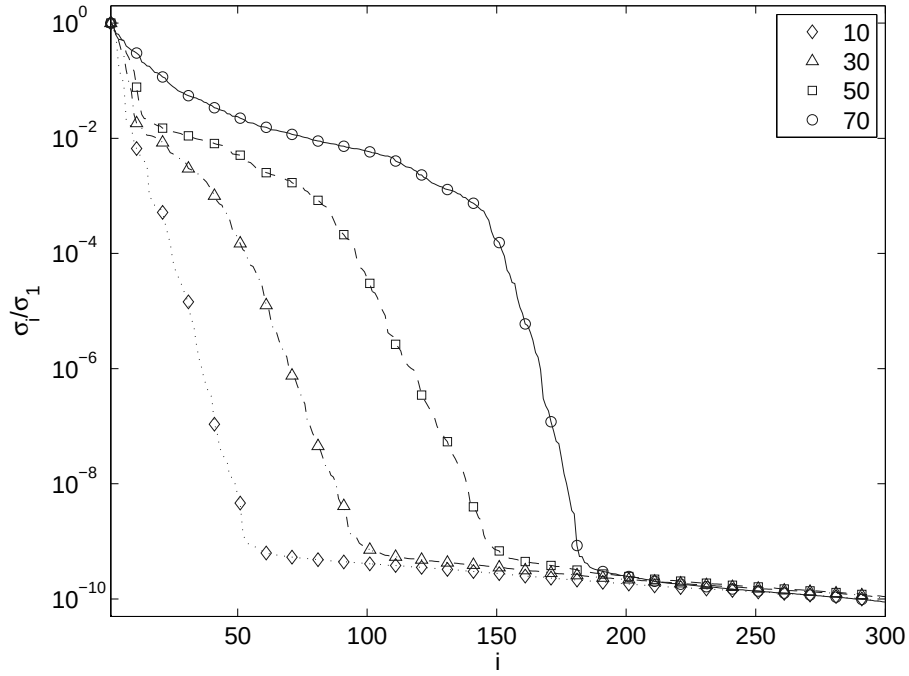

Figure 5. The normalised singular values, σ_i/σ_1, for different incident angle ranges. All plots have 200 incident angles in the range -θ to θ.

information. Liquid crystals are highly birefringent and the ray approximation cannot be used, the problem cannot be reduced in this way. Figures 6 and 7 show the normalized singular values plotted for different values of the birefringence, Δn. As Δn becomes small the number of singular vectors that can be used to construct a solution drops to five, even with a large angle range. This is expected from the truncated transverse ray transform (see for example, Chapter 6 in Sharafutdinov [16]).

6. Theoretical details

While the numerical studies we have presented stand on their own, there are some limited theoretical results that are also illuminating. First we show how the linearization of the Berreman equations, and consequently the Jacobian J, can be derived without recourse to a finite difference approximation perturbing parameter values. We begin with the Berreman system of ODEs in the form

$$\left(\frac{d}{dz} + \frac{\mathrm{i}\omega}{c} M_\xi\right) X_\xi = h \tag{24}$$

for some fixed ξ. Of course $h = 0$ in Berreman's equations but we will have cause to solve for non-zero $h(z)$ in the course of our linearization. For clarity we omit the ξ subscripts in what follows. We note that there is a Green's function G so that the

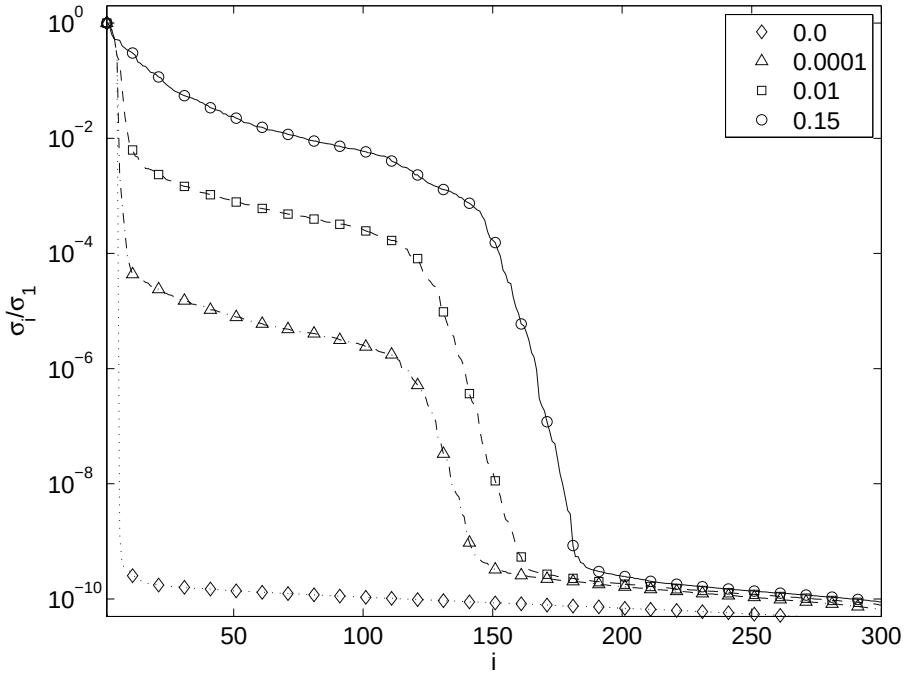

Figure 6. The normalised singular values, σ_i/σ_1, for different values of the birefringence, Δn.

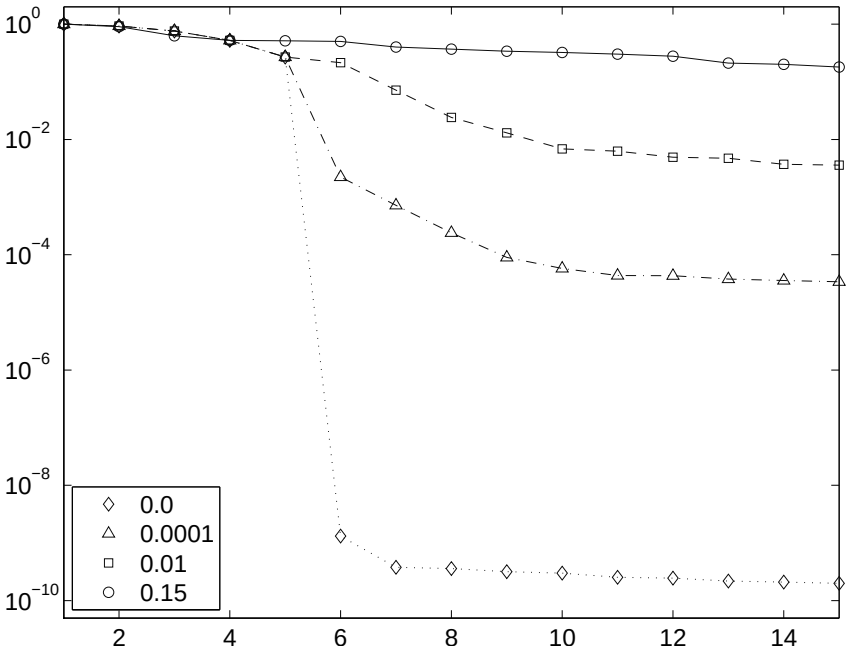

Figure 7. Detail from figure 6 showing the collapse to just five singular values when the birefringence goes to zero. In this plot all of the points are marked.

solution to (24) can be written

$$X(z) = P(z)X(0) + \int_0^z G(z,z')h(z')dz' \tag{25}$$

and we shall write the right most term in operator notation as $\mathcal{G}[h]$. Now we consider a hypothetical perturbation of the material parameters resulting in a change in the Berreman matrix to $M_\xi + \delta M_\xi$. For simplicity we will assume the initial condition $X(0)$ is fixed and, although in our practical situation that is not the case, we will rectify the deficiency below. Taking M to be an initial guess, and h in (24) to be 0, the new electromagnetic field $X + \delta X$, with $\delta X(0) = 0$, satisfies

$$\left(\frac{d}{dz} + \frac{\mathrm{i}\omega}{c}(M + \delta M)\right)(X + \delta X) = 0 \tag{26}$$

or

$$\left(\frac{d}{dz} + \frac{\mathrm{i}\omega}{c}M\right)\delta X = \frac{\mathrm{i}\omega}{c}(\delta M X + \delta M \delta X) \tag{27}$$

using (24). We see that this is a differential equation of the same form as (24) but in δX, and in operator form is

$$\left(1 - \frac{\mathrm{i}\omega}{c}\mathcal{G}\delta M\right)[\delta X] = \frac{\mathrm{i}\omega}{c}\mathcal{G}[\delta M X]. \tag{28}$$

Using the standard Neumann series for operators we can write

$$\left(1 - \frac{\mathrm{i}\omega}{c}\mathcal{G}\delta M\right)^{-1} = 1 + \frac{\mathrm{i}\omega}{c}\mathcal{G}\delta M + (\frac{\mathrm{i}\omega}{c}\mathcal{G}\delta M)^2 + \cdots \tag{29}$$

a series that will converge provided the operator norm $\|\frac{\omega}{c}\mathcal{G}\delta M\| < 1$, which can be ensured by taking a sufficiently small perturbation in δM. We now see that to first order in δM

$$\delta X = \mathcal{G}[\delta M X] \tag{30}$$

or returning to the differential form

$$\left(\frac{d}{dz} - \frac{\mathrm{i}\omega}{c}M\right)\delta X = \frac{\mathrm{i}\omega}{c}\delta M X \tag{31}$$

to first order. The final data is obtained by solving this ODE for its final value $\delta X(d)$, or from the integral

$$\delta X(d) = \frac{\mathrm{i}\omega}{c}\int_0^d G(d, z)\delta M(z)X(z)dz. \tag{32}$$

In our practical application M depends on the parameters for each layer, but the dependence is a simple algebraic formula that can easily be differentiated, so the partial derivatives of the final value $X_\xi(d)$ with respect to each parameter is readily calculated using the chain rule.

Let us pause to consider what type of inverse problem we have. ξ depends on the incident angle and enters the formula for M (see (13)) as terms up to second order. If M was simply a linear function of ξ we would have something very close to the inverse Sturm-Liouville problem of recovering the coefficients of an operator from its boundary eigendata. Indeed before the elimination of the z components of the electric and magnetic field we had a 6×6 system of second order partial differential equations

where the coefficient matrix is linear in ξ. Similar, but not identical inverse spectral problems are treated for example by [14, 15]. Just as in typical inverse spectral problems our boundary data is an analytic function of ξ so for exact data a knowledge of $X_\xi(d)$ for ξ in some interval is sufficient to determine the data for all ξ by analytic continuation. However analytic continuation is extremely ill-posed so we expect that in numerical examples a wider range of incident angles will result in a better conditioned system.

We can explore this phenomenon in a little more depth, and provide some insight in to the numerical results, by considering perturbation about a homogeneous M. In this case we have an explicit formula for the Green's function and find that the solution for (24) is

$$X(z) = \exp(\frac{\mathrm{i}\omega}{c}Mz) \times \left(\int_0^z \exp(-\frac{\mathrm{i}\omega}{c}Mz')h(z')dz' + X(0) \right) \tag{33}$$

or $G(z,z') = \exp(-\mathrm{i}\omega(z-z')M/c)$ so that (32) becomes

$$\delta X(d) = \frac{\mathrm{i}\omega}{c}\exp(-\frac{\mathrm{i}\omega}{c}Md) \times \int_0^d \exp(\frac{\mathrm{i}\omega}{c}Mz)\delta M(z)\exp(-\frac{\mathrm{i}\omega}{c}Mz)X(0)dz. \tag{34}$$

As for non-lossy materials M is real, we can consider (34) as a generalized Fourier transform of δMX. The successful recovery of the unknown spatially varying coefficients in δM relies on knowing their moments with respect to a sufficiently large range of functions. Here ξ plays a role analogous to a frequency variable and it is reasonable to expect that a wider range of incident angles would yield more information. The eigenvalues q_i of M, are typically distinct and for non-dissipative media are real. Let U be the matrix of eigenvectors of M, and $Q = \mathrm{diag}(q_i)$ so that (34) becomes

$$\delta X(d) = \exp(\frac{\mathrm{i}\omega}{c}Md) \times \int_0^d U\exp(-\frac{\mathrm{i}\omega}{c}Qz)A\exp(\frac{\mathrm{i}\omega}{c}Qz)U^{-1}X(0)dz \tag{35}$$

with $A = U^{-1}\delta M(z)U$.

We note that $\exp(-\frac{\mathrm{i}\omega}{c}Qz)A\exp(\frac{\mathrm{i}\omega}{c}Qz)$ has elements $e^{i(q_i-q_j)z}A_{ij}$. As we know all possible pairs of initial and final data $X(0), X(d)$, we know the linear response map T defined by $\delta X(d) = TX(0)$. From this data, and the known initial orthorhombic ϵ we also know the matrix

$$Y = \exp(-\frac{\mathrm{i}\omega}{c}Md)U^{-1}TU = \int_0^d \exp(-\frac{\mathrm{i}\omega}{c}Qz)A\exp(\frac{\mathrm{i}\omega}{c}Qz)\,dz \tag{36}$$

and so

$$Y_{ij} = \int_0^d e^{\frac{\mathrm{i}\omega}{c}(q_i-q_j)z}A_{i,j}dz = \widehat{A_{i,j}}(q_i-q_j) \tag{37}$$

where the $\hat{}$ denotes the Fourier transform and A is considered to be extended by zero outside the interval $[0, d]$. Here the q_i are functions of ξ and in general varying ξ over an interval will vary $q_i - q_j$ over an interval, for $i \neq j$. We see therefore that this data, over a variety of incident angles gives us some information about the deviation of the permittivity tensor from our initial constant assumption, in terms of the deviation of the measurements from those we could calculate for the constant case.

If it were not for the awkward fact that U is also a function of ξ, we could invoke the Paley-Wiener theorem that says that the Fourier transform of a compactly supported function is entire. Knowing an entire function on an interval is enough to determine the Taylor series, and hence the function everywhere. However such analytic continuation is severely ill-posed, and we can expect our problem to be as well. In simple cases we can expect to calculate U explicitly and come to a definite conclusion about the sufficiency of data for the linearized problem, and an example of this is given in the next section.

7. Orthorhombic case

Following Berreman we attempt to understand one of the simplest cases. We consider a general perturbation in permittivity tensor δ about the permittivity for an orthorhombic crystal with principle axes aligned with the coordinate axes. As before we take the incident plane to be the xz plane.

For the orthorhombic case M reduces to

$$\begin{pmatrix} 0 & \mu_0 c\frac{\epsilon_{33}-\xi^2}{\epsilon_{33}} & 0 & 0 \\ \epsilon_0 c\epsilon_{11} & 0 & 0 & 0 \\ 0 & 0 & 0 & \mu_0 c \\ 0 & 0 & \epsilon_0 c\left(\epsilon_{22}-\xi^2\right) & 0 \end{pmatrix}$$

The eigenvalues are

$$q_1 = \sqrt{\frac{\epsilon_{11}}{\epsilon_{33}}}\sqrt{\epsilon_{33}-\xi^2},\ q_2 = -q_1,\ q_3 = \sqrt{\epsilon_{22}-\xi^2},\ q_4 = -q_3$$

with matrix of eigenvectors

$$U = \begin{pmatrix} -\frac{q_1}{c\epsilon_0\epsilon_{11}} & \frac{q_1}{c\epsilon_0\epsilon_{11}} & 0 & 0 \\ 1 & 1 & 0 & 0 \\ 0 & 0 & -c\mu_0/q_3 & c\mu_0/q_3 \\ 0 & 0 & 1 & 1 \end{pmatrix}$$

and inverse

$$\begin{pmatrix} -c\epsilon_0\epsilon_{11}/2q_1 & \frac{1}{2} & 0 & 0 \\ c\epsilon_0\epsilon_{11}/2q_1 & \frac{1}{2} & 0 & 0 \\ 0 & 0 & \frac{-q_3}{2\,c\mu_0} & \frac{1}{2} \\ 0 & 0 & \frac{q_3}{2\,c\mu_0} & \frac{1}{2} \end{pmatrix}$$

We calculate the perturbation δM corresponding to $\epsilon + \delta$

$$\delta M = \begin{pmatrix} -\frac{\xi\,\delta_{13}}{\epsilon_{33}} & \frac{\xi^2\,\delta_{33}}{c\epsilon_0\epsilon_{33}^2} & -\frac{\xi\,\delta_{23}}{\epsilon_{33}} & 0 \\ c\epsilon_0\delta_{11} & -\frac{\xi\,\delta_{13}}{\epsilon_{33}} & c\epsilon_0\delta_{12} & 0 \\ 0 & 0 & 0 & 0 \\ c\epsilon_0\delta_{12} & -\frac{\xi\,\delta_{23}}{\epsilon_{33}} & c\epsilon_0\delta_{22} & 0 \end{pmatrix}$$

and then consider the coefficient of each δ_{ij} in $U^{-1}\delta MU$, noting that we will be able to obtain Fourier data for off-diagonal terms.

$$\text{coefficient of } \delta_{11} = \frac{q_3}{2c\epsilon_0\epsilon_{11}} \begin{pmatrix} -1 & 1 & 0 & 0 \\ -1 & 1 & 0 & 0 \\ 0 & 0 & 0 & 0 \\ 0 & 0 & 0 & 0 \end{pmatrix}$$

$$\text{coefficient of } \delta_{12} = \frac{1}{2c\epsilon_0} \begin{pmatrix} 0 & 0 & -\frac{1}{q_3} & \frac{1}{q_3} \\ 0 & 0 & -\frac{1}{q_3} & \frac{1}{q_3} \\ -\frac{q_1}{2\epsilon_{11}} & \frac{q_1}{2\epsilon_{11}} & 0 & 0 \\ -\frac{q_1}{2\epsilon_{11}} & \frac{q_1}{2\epsilon_{11}} & 0 & 0 \end{pmatrix}$$

$$\text{coefficient of } \delta_{13} = -\frac{\xi}{c\epsilon_0\epsilon_{33}} \begin{pmatrix} 1 & 0 & 0 & 0 \\ 0 & 1 & 0 & 0 \\ 0 & 0 & 0 & 0 \\ 0 & 0 & 0 & 0 \end{pmatrix}$$

$$\text{coefficient of } \delta_{22} = \frac{c\mu_0}{2q_3} \begin{pmatrix} 0 & 0 & 0 & 0 \\ 0 & 0 & -1 & 1 \\ 0 & 0 & -1 & 1 \end{pmatrix}$$

$$\text{coefficient of } \delta_{23} = \begin{pmatrix} 0 & 0 & -\frac{\xi\sqrt{\epsilon_{11}}}{2\sqrt{\epsilon_{33}}q_1q_3} & \frac{\xi\sqrt{\epsilon_{11}}}{2\sqrt{\epsilon_{33}}q_1q_3} \\ 0 & 0 & \frac{\xi\sqrt{\epsilon_{11}}}{2\sqrt{\epsilon_{33}}q_1q_3} & -\frac{\xi\sqrt{\epsilon_{11}}}{2\sqrt{\epsilon_{33}}q_1q_3} \\ -\frac{\xi}{2\epsilon_{33}} & -\frac{\xi}{2\epsilon_{33}} & 0 & 0 \\ -\frac{\xi}{2\epsilon_{33}} & -\frac{\xi}{2\epsilon_{33}} & 0 & 0 \end{pmatrix}$$

$$\text{coefficient of } \delta_{33} = \frac{\xi\epsilon_{11}}{2\epsilon_{33}q_1} \begin{pmatrix} -1 & -1 & 0 & 0 \\ 1 & 1 & 0 & 0 \\ 0 & 0 & 0 & 0 \\ 0 & 0 & 0 & 0 \end{pmatrix}$$

We see that for all except δ_{13} there are non-trivial off diagonal components so that for data using incident light in this plane for an interval of incident angles the Fourier transforms of all other δ_{ij} are determined for some interval of frequencies, hence by analytic continuation the perturbation is determined uniquely everywhere. Although of course their recovery in the presence of noise will be unstable. Note now that by rotating the plane of incidence through a right angle, the x and y axis swap roles and

we can with the data for these two planes recover all the perturbed coefficients. Now let us look in a little more detail at the off diagonal terms above. For each of the identifiable δ_{ij} we recover $P_\xi \hat{\delta}_{ij}(q_i(\xi) - q_j(\xi))$ where P_ξ is either a known constant or a known multiple of ξ or $q_k^{\pm 1}$ or ξ/q_k for $k = 1$ or 3. In any case these are Fourier integral operators applied to δ_{ij}. One can expect different spectral information on δ_{ij} from a term appearing in the 1 2 or 3 4 position from those in the 1 3 and 2 4 positions. In the first case $q_1 - q_2 = 2q_1, q_3 - q_4 = 2q_3$, and as $dq_i/d\xi = 0$ at $\xi = 0$ a small range of incident angle about zero gives only a small spectral window. By contrast q_1 and q_3 will be close for a weakly anisotropic medium, indeed for $\epsilon_{11} = \epsilon_{22}$

$$q_1 - q_3 = \frac{\sqrt{\epsilon_{11}}}{2}\left(\frac{1}{\epsilon_{11}} - \frac{1}{\epsilon_{33}}\right)\xi^2 + O(\xi^4)$$

giving a wider spectral window for a range of incident angles near zero.

8. An alternative approach

Researchers in the Department of Physics at the University of Exeter have been working on similar problems for some time [1, 2, 3, 4]. Figure 8 shows the experimental setup that they use. Instead of a cylindrical mount Exeter use prisms to allow high angles of incidence to be achieved, although this does restrict the incident angle range over which measurements can be taken. For each incident angle s and p polarized light is input and the reflected and transmitted intensities for s and p polarizations are measured♯. This gives eight measurements for each incident angle: R_{ss}, R_{sp}, R_{ps}, R_{pp}, T_{ss}, T_{sp}, T_{ps} and T_{pp}. We have carried out a similar analysis for the Exeter experiment, assuming that

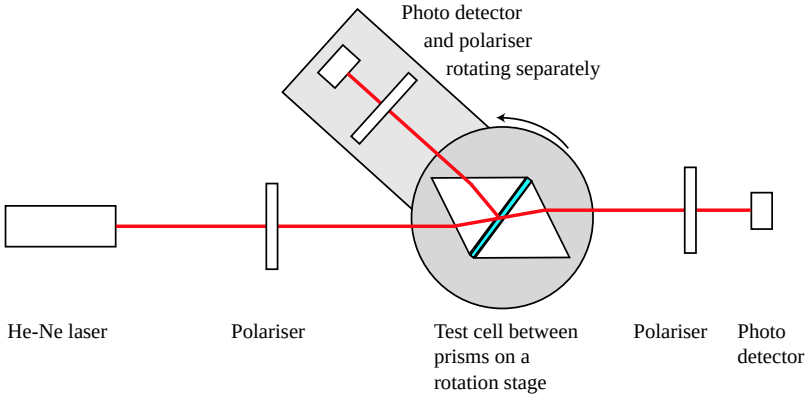

Figure 8. The experimental setup used at Exeter University. The photo detector and polarizer for the reflected beam rotate at twice the speed of the cell.

the azimuthal angle for the cell is 45^o and that the range of incident angles used is the same as in a typical experiment $(60 - 72^o)$. The results for the different test director profiles are shown in figure 9. The distribution of singular values is very similar and so

♯ The liquid crystal cell is inserted in the beam with the director out of the incident plane to ensure that there is some polarization conversion.

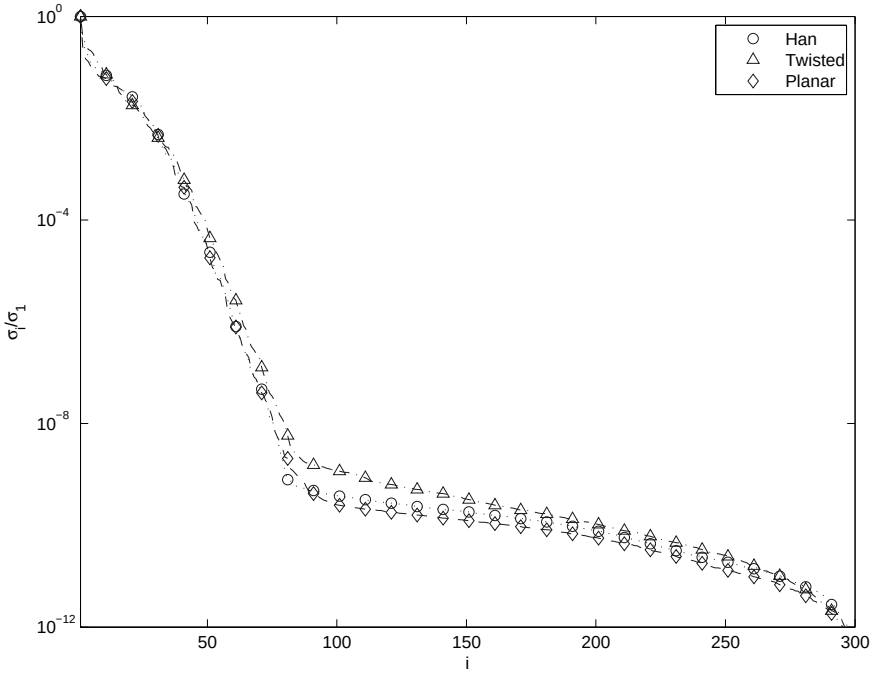

Figure 9. The normalised singular values, σ_i/σ_1, for the Exeter experiment and different initial parameter configurations, p_0.

their problem is equally ill-posed. Any methods developed to facilitate the solution of our inverse problem should work in this case also.

9. Conclusions

Our numerical investigation shows that a dielectric tensor depending on depth can be recovered from the experimental measurements used by both the HPLB and Exeter groups. While there is no rank deficiency indicating a unique solution for exact data, this is a severely ill posed problem so some regularization will be needed to recover the dielectric tensor field from experimental data. The number of parameters that can be recovered for a given data error increases as the range of incident angle is increased.

In a special case of a general perturbation of an orthorhombic material, the linearized inverse problem has a unique solution, provided two planes of incidence are used. Further work is needed to apply the techniques of inverse spectral theory for systems of ordinary differential equations to this problem in an attempt to understand the question of sufficiency of data more completely.

Some simplification of the inverse problem can be obtained by assuming that the LC is uniaxial (in inverse problem terms this is the inclusion of prior information). We can also use the Euler-Lagrange equations obtained by minimizing the free energy (1) to constrain any solution. Results for this uniaxial case, efficient methods of solving the inverse problem using the Euler-Lagrange equations and results using experimental

data will be reported separately.

A more general problem where we remove the hypothesis that the medium is stratified has been treated numerically using the finite element method for forward solution and is reported in [17]. The question of sufficiency of data for this more general case is still an open problem.

Acknowledgments

The authors would like to thank Roy Sambles and Timothy Spiller for useful discussions. This work was sponsored by the Smith Institute Faraday Partnership and supported by EPSRC grant GR/R93612/01.

Appendix

The Berreman method gives us

$$X_t = P(X_i + X_r)$$

Following Galatola and Oldano [18] we rewrite this in terms of the TM and TE components of the electric fields on the beams. So we have

$$X_i + X_r = T_1 \begin{pmatrix} i_1 \\ i_2 \\ r_1 \\ r_2 \end{pmatrix}$$

with

$$T_1 = \begin{pmatrix} \cos\theta_i & 0 & -\cos\theta_i & 0 \\ \epsilon_0 c n_1 & 0 & \epsilon_0 c n_1 & 0 \\ 0 & 1 & 0 & 1 \\ 0 & \epsilon_0 c n_1 \cos\theta_i & 0 & -\epsilon_0 c n_1 \cos\theta_i \end{pmatrix}$$

Similarly, assuming that there is only an outgoing transmitted wave, we can write

$$X_t = T_2 \begin{pmatrix} t_1 \\ t_2 \\ 0 \\ 0 \end{pmatrix}$$

with

$$T_2 = \begin{pmatrix} \cos\theta_t & 0 & -\cos\theta_t & 0 \\ \epsilon_0 c n_2 & 0 & \epsilon_0 c n_2 & 0 \\ 0 & 1 & 0 & 1 \\ 0 & \epsilon_0 c n_2 \cos\theta_t & 0 & -\epsilon_0 c n_2 \cos\theta_t \end{pmatrix}$$

We then have

$$T_2 \begin{pmatrix} t_1 \\ t_2 \\ 0 \\ 0 \end{pmatrix} = PT_1 \begin{pmatrix} i_1 \\ i_2 \\ r_1 \\ r_2 \end{pmatrix}$$

giving

$$\begin{pmatrix} t_1 \\ t_2 \\ 0 \\ 0 \end{pmatrix} = U_B \begin{pmatrix} i_1 \\ i_2 \\ r_1 \\ r_2 \end{pmatrix}$$

with $U_B = T_2^{-1} P T_1$. Defining the projection matrices

$$P_+ = \begin{pmatrix} 1 & 0 & 0 & 0 \\ 0 & 1 & 0 & 0 \\ 0 & 0 & 0 & 0 \\ 0 & 0 & 0 & 0 \end{pmatrix}$$

and

$$P_- = \begin{pmatrix} 0 & 0 & 0 & 0 \\ 0 & 0 & 0 & 0 \\ 0 & 0 & 1 & 0 \\ 0 & 0 & 0 & 1 \end{pmatrix}$$

we can rewrite the equation as

$$\begin{pmatrix} t_1 \\ t_2 \\ r_1 \\ r_2 \end{pmatrix} = (P_+ - U_B P_-)^{-1} U_B \begin{pmatrix} i_1 \\ i_2 \\ 0 \\ 0 \end{pmatrix}$$

So, given the TM and TE components of the incident wave we can calculate the TM and TE components of the transmitted and reflected waves.

References

[1] D.Y.K. Ko and J. R. Sambles, J. Opt. Soc. Am., A**5**, 1863 (1988).
[2] N.J. Smith and J. R. Sambles, J. Appl. Physics, **85**, 3984 (1999).
[3] B. T. Hallam, F. Yang and J. R. Sambles, Liquid Crystals, **26**, 657 (1999).
[4] A. Mazzulla, F. Ciuchi and J. R. Sambles, Phys. Rev. E, **64**, 21708 (2001).
[5] B.A. Robson, *The Theory of Polarisation Phenomena*, Clarendon Press, Oxford (1974).
[6] D. W. Berreman, J. Opt. Soc. Am. **62**, 502 (1972).
[7] A. Lien, Liquid Crystals **22**, 171 (1997).
[8] R. P. Feynman and R. B. Leighton and M. Sands, *Lectures on Physics, Volume 2*, Addison-Wesley (1989)
[9] L. N. Trefethen and D. Bau III, *Numerical Linear Algebra*,SIAM (1997)
[10] G. H. Golub and C. F. Van Loan, *Matrix Computations*,The John Hopkins University Press (1996)
[11] C. V. Brown, G. P. Bryan-Brown and V. C. Hui, Proc. 16th ILCC, (1997).

[12] C. J. P. Newton and T. P. Spiller, Proc International Displays Research Conference (SID), 13 (1997).
[13] P. G. de Gennes and J. Prost, *The Physics of Liquid Crystals*, 2nd ed. OUP, Oxford (1993).
[14] P.J. Caudrey, Physica D, **6**, 51-66, (1982).
[15] L. Sakhnovich, Inverse Problems, **18**, 1525-1536 (2002).
[16] V. A. Sharafutdinov, Integral Geometry of Tensor Fields, VSP, Netherlands, 1994.
[17] N Polydorides, Electromagnetic inverse problems for nematic liquid crystals and capacitance imaging. preprint 2004.
[18] P. Galatola and C. Oldano, *The Optics of Thermotropic Liquid Crystals, Eds. Elston and Sambles* Chapter 3, Taylor and Francis (1998)